Journal Homepage: http://ijcpe.uobaghdad.edu.iq
Iraqi Journal of Chemical and Petroleum Engineering
Vol. 25 No. 3 (September 2024) 1 – 14
EISSN: 2618-0707, PISSN: 1997-4884

Reservoir and rock characterization for Mishrif Formation/ Zubair Field (Rafdiya and Safwan Domes) by nuclear magnetic resonance and cores analysis

Ahmed N. Al-Dujaili [a, *]

a Petroleum Engineering Department, Amirkabir University of Technology, Iran

Abstract

The identification studies of rock and reservoir characteristics are essential for evaluating the efficiency of a reservoir by analyzing the types of rock and pores. In this study, Nuclear Magnetic Resonance (NMR) for six wells was utilized to identify the rock and reservoir characteristics of the Mishrif formation in the South of the Zubair Field, specifically the Rafdyia and Safwan domes, as well as the west flank. Specific correlations were utilized to describe the classification of rocks, estimate pore throat radius, and recognize possible flow intervals. The results revealed that the Mishrif Formation mainly consists of limestone, dolomite, and shale. The Safwan dome consists mainly of pack-wackestone, wackestone, and mudstone, while the Rafdyia dome is a mixture of packstone, grainstone, and wackestone with some shoal and rudist bioherm facies. The west flank is characterized by pack-wackestone, wackestone, and mudstone. These results were further supported by core analysis. Pore throat types in the Safwan dome range from Micropores to Nanopores, while the Rafdyia dome is dominated by Megapores, Macropores, and Mesopores. The back-shoal facies overwhelm the packstone microfacies. The west flank of the Mishrif Formation in the Zubair Field is mesoporous and micropores. Flow units were identified in the Safwan and Rafdyia domes, as well as the west flank. The Safwan dome has fifteen flow units in the north and seven in the south, while the Rafdyia dome has ten flow units in both the north and south regions, with five flow units on the west flank of the Zubair Field.

Keywords: Reservoir Characterization; NMR; Rafdyia and Safwan Domes; Mishrif Formation; Zubair Field.

Received on 28/02/2024, Received in Revised Form on 08/06/2024, Accepted on 08/06/2024, Published on 30/09/2024

https://doi.org/10.31699/IJCPE.2024.3.1

1- Introduction

The number of pore spaces in the rocks can indicate the characteristic of porosity [1], while the rock's capability to move fluids through the formation refers to permeability [2]. The evaluation of Reservoir and rock characterizations by forenamed petrophysical characteristics is an indisputable function and, consequently, the first stage to expand the production, and development strategies of the Field. The porosity of rocks can be determined directly in the Lab [3], and it can be accomplished in varied forms, but the designation of the permeability is challenging according to many causalities, so specialists have made many endeavors to evaluate permeability by indirect methods [4].

Various procedures have been supplied to measure the permeability, such as area-specific surface [5], the formation of grains [6], the pores form [7], and the size of grains [8]. The benefit of suggested procedures is the heightened accuracy of estimation, and their essential drawback is the requirement of additional core samples and complex laboratory examinations. These correlations can be relatable with strict problems according to mixed grounds, like the absence of access to core samples (mainly in the horizontally drilled wells), the heightened expenditure, and the prolonged operation time.

The explicit principle of Nuclear Magnetic Resonance (NMR) is that the magnetic domain is affected by molecular demeanor [9]. If the nuclei are considered as bar magnets, this will be the most acceptable model for clarifying this demeanor to align it with magnetic characteristics in a magnetic domain [9]. The two significant properties of the nuclear rod magnets are the magnetic moment, which determines the power of the relations, and the second is the spin located in the magnetic domain and the nuclei whirl, which forces the nuclear bar magnet to rotate around the magnetic field.

NMR is to be welfare in the formation evaluation according to the demeanor of the nuclear spins, which is related to the effect of the fluid characteristics (notably the chemical composition) and the fluid viscosity. NMR technology is operated specifically to define various characterizations of rocks and fluids, including (porosity, kind of fluid, pore size allocation, and permeable rocks characteristics) [10-14]. By NMR technology, it is possible to estimate porosity, but permeability cannot be

*Corresponding Author: Email: ahmed.noori203@aut.ac.ir

estimable directly. Thus, periodic procedures have been utilized to evaluate permeability [12]. It has been examined adequately in sandstone formations; consequently, it is achievable to specify additional parameters, including porosity, Bulk Volume Movable (BVM), Bulk Volume Irreducible (BVI), and permeability in sandstones (10, 15]. Nonetheless, the circumstances are different in carbonate rocks.

The NMR measurement utilized in the petrophysical analysis of rocks uses three different applied magnetic fields [16]:

1. B0, which represents a static magnetic domain.
2. B1 is a magnetic domain generated by oscillating radio frequency pulses. This domain is laid (Normally at right angles) to the static B0.
3. Local magnetic domain fluctuations can be inducible by unpaired electrons and bordering nuclei.

Detection of magnetization decay in the transverse plane is known as "transverse relaxation" or "T2 relaxation". In the case of formation evaluation, the NMR investigation essentially explores the time it carries for the protons' spins to relax from B1 to B0 by catching magnetization in the transverse plane [17].

1.1. Time of y-z versus time of x-y plane Relaxation

The time assumed for the proton spins to transmit from a random alignment to grow in the trend of the B0 domain represents T1 relaxation [18]. The proton spins in the transverse planer are associated with the relaxation of T2 that aligned with the B1 domain. T2 is in the normal trend of B0 and parallel to B1 (in other words, T1 indicates the y-z plane and T2 the x-y plane) [19].

The variation between T1 and T2 can be assumed as the estimation of relaxation to B0 in two different trends. T1 ricochets in trend of B0 and it will be normal to B1. The allocation of exponentials or T2 distribution can be interpreted in terms of pore size and the fluid composition residing in the pore [20].

1.2. Rock types

Pore systems are identified as displayed in the structure of the particular deposits [21-23]. Lucia's technique depends on the sedimentological and diagenesis possibility with physical characterizations depending on Archie's anthology [24], which consists of three major pore types, where rocks are recognized into types with the same deposition essentials and diagenesis identically [25]. The main factors affecting rock types are Pore size, porosity, sorting, and separate vugs porosity. According to Lucia, rock types can be identified in classes 1, 2, and 3 (Table 1).

Lucia's rocks fabric number (RFN) can be represented in Eq. 1.

$$Log\ k = \{9.7982 - 12.0803\ log(RFN) + [8.6711 - 8.2965\ log(RFN)]\ log\ \varphi\} \quad (1)$$

Where: K= permeability (millidarcy). RFN = the rock's fabric number (dimensionless). φ = Porosity (fraction).

Table 1. Rock Types [25]

Category #	Grain size µm	type of rock	Influenced characteristics
1	> 100	basically Grainstone	size of grains, grain classification, and inter-grain cement bonding
2	20–100	Prevailing is Packston	Size of grains, micrite between grains, and cement bonding.
3	< 20	Mainly Pack-wackestone, in addition to Wackestone, and Mudstone.	Porosity between the grains and micrite grain size

1.3. Pore throat radius

Winland examined pores interconnecting with a Mercury saturation of 35% (registered as r35) for a set of core plugs of sandstones and carbonate [26]. The regression at (30, 40, and 50% of saturation) was estimated also, and the best value was at 35% (Eq. 2). There is no justification for why 35% resulted in the best correlation. A classification of pore throat types was adopted according to the Winland equation [26] as shown in Table 2.

$$Log\ 35 = \{0.732 + 0.588\ log(k_{air}) - 0.864\ log\ \varphi\} \quad (2)$$

Table 2. Types of Pore Throat According to [26]

Type	Radius in microns
Megapores	> 10
Macropores	2.5 - 10
Mesopores	0.5 - 2.5
Micropores	0.2 - 0.5
Nanopores	< 0.2

1.4. Flow units

It is a portion of the reservoir where the characteristics (including petrophysical and geological) are regular and prognosticated by other rock characteristics, and it can control fluid flow [28]. It is "the stratigraphically continued separation of a similar reservoir that follows the geological formation and bears the same rock characteristics" In simple words (same porosity, permeability, and bed thickness values) [29]. Various methods have been designed to identify flow units depending on different parameters, like descriptions of pore geometry, a depositional environment of rock structure, and a diagenetic process. The Reservoir quality index (RQI) and Flow zone indicator (FZI) can directly specify flow units [30]. RQI and FZI can be identifiable by the following equations [21, 31]:

$$RQI\ (\mu m) = 0.0324\left(\sqrt{K_/\ \varphi_e}\right) \quad (3)$$

$$FZI = RQI\ (\varphi z) \quad (4)$$

$$\varphi z = \left(\frac{\varphi_e}{(1-\varphi_e)}\right) \quad (5)$$

2- Geological setting

Zubair oilfield lies back in the Mesopotamian zone within an unstable sill of the Arabian Platform [32]. Zubair is one of the mature oilfields in southern Iraq, located 20 km southwest of Basra city (Fig. 1) [33]. This field was discovered in 1949 [34] consisting of four domes (Al-Hamar, Shuaiba, Rafdyia) in the NW and (Safwan) to the SE communicated with each other through an aquifer extending beyond the Iraqi and Kuwaiti border [35].

The stratigraphic column of southern Iraq [36, 37] characterized a thick Cretaceous depositional sequence with significant hydrocarbon accumulations within many formations [38] (Fig. 2). The field structure includes four reservoirs, Mishrif, Upper Shale Member, third Pay, and fourth Pay [39]. Zubair and Mishrif Formations represent two main productive reservoirs in southern Iraq.

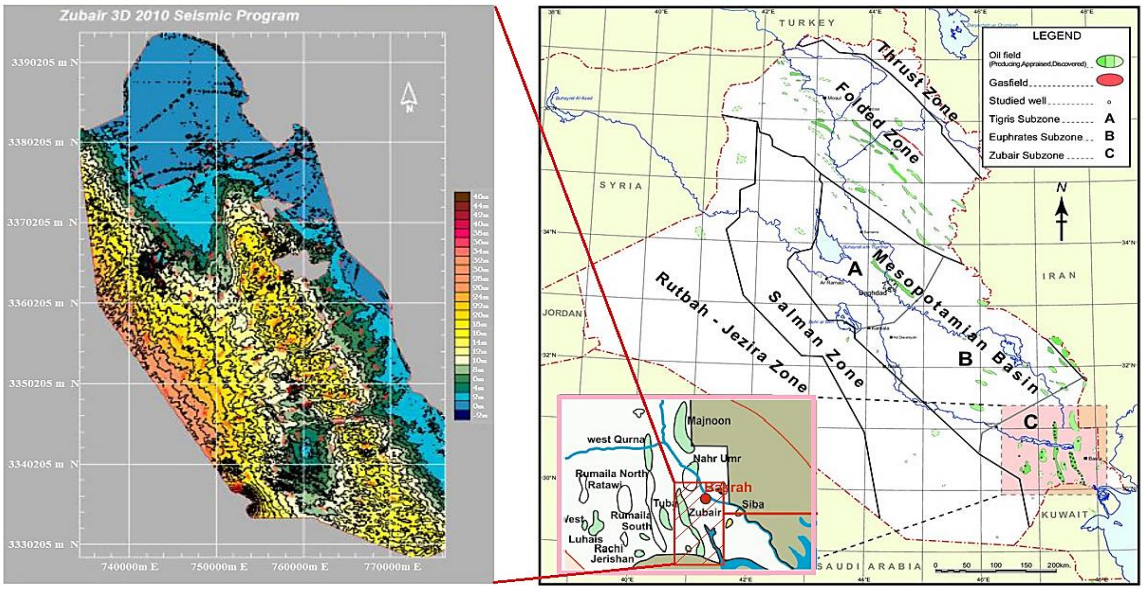

Fig. 1. Zubair Oilfield Location [33]

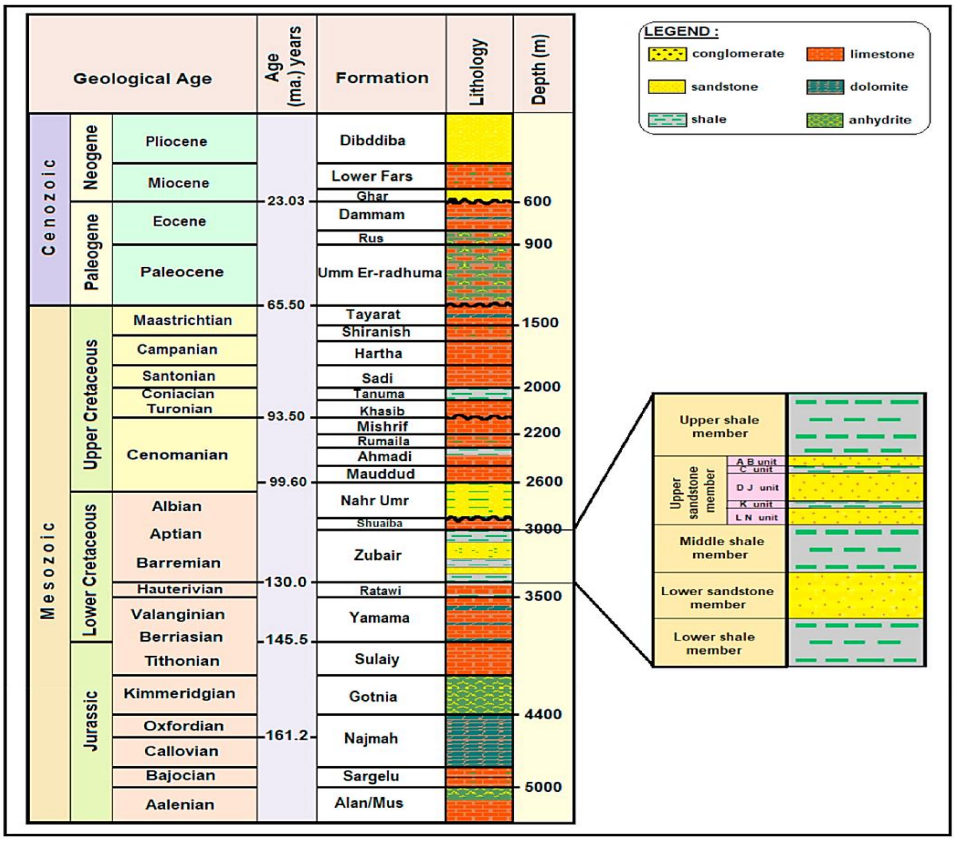

Fig. 2. Stratigraphic Column in Southern Iraq [36, 37]

Mishrif Carbonate reservoir and upper and lower Sandstone reservoirs depositional period are Middle and Lower Cretaceous. Mishrif Reservoir is present only in the northeast of the field in two domes (Hammar and Shuaiba), while changes in facies occur towards the south. Similarly, to most Iraqi fields, the petroleum system of the Zubair Field is dominated by the late Mesozoic (Mishrif) warming and shallow. Salt tectonics generally is the main driving force behind the formation of stable shelf region structures in Iraq. The northern part of the field has been affected more by this event, as can be noticed by increased relief of the Al-Hamar and Shuaiba domes compared to the southern Rafdyia dome region.

There is minimal evidence of Zagros orogeny imprint even though the field is located south of the Mesopotamian Foredeep Basin, away from the Zagros fold belt.

2.1. Mishrif reservoir

Mishrif Formation is separable according to the well-known unconformity into two big extended regressive successions, significantly distinguishable in the east of the Mesopotamian Basin. Considerable intervals are attended in both sequences [40]. The west of the Basin is overwhelmed by the Lower Sequence, which has relatively few reservoir intervals. The shallow water in the east is thicker than reflects high subsidence rates throughout the Cenomanian era. The subsidence rates on the western side of the Basin were lower. Moreover, it is noticeable that all reservoir units are thinner and more limited [23]. The most satisfactory reservoir conditions for Mishrif are represented clearly in the rudist-bearing facies, such as rudstone and the rudist packstone/ grainstone [41] (Fig. 3).

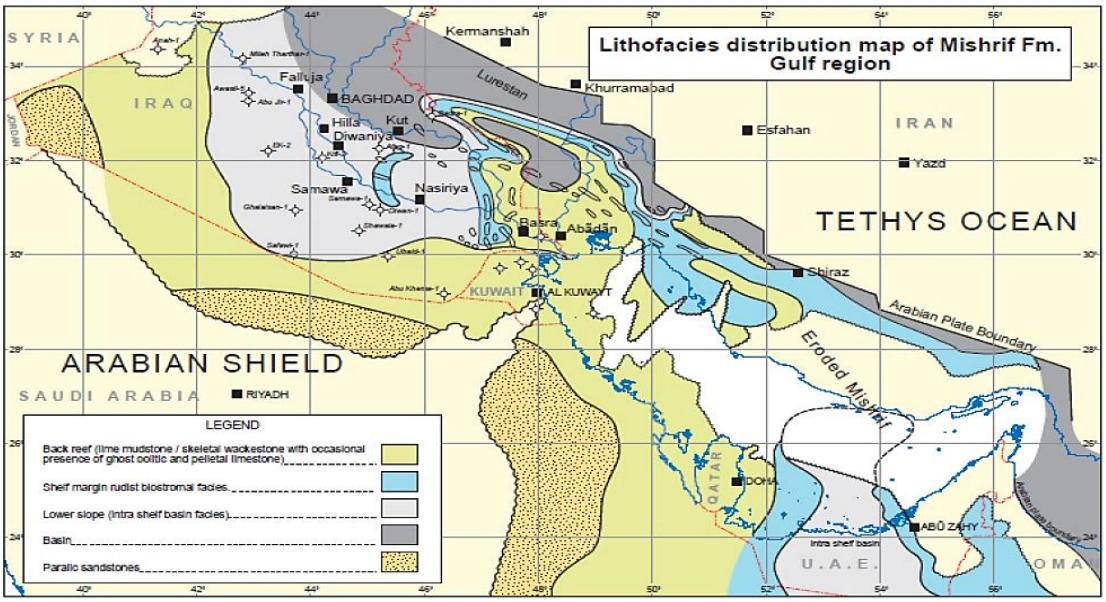

Fig. 3. Lithofacies Distribution Map of the Mishrif Formation, Gulf Region [41]

3- Data and methods

Wireline and core data were utilized for six wells in the Mishrif Formation at the Zubair oilfield, with two wells in each of the Rafdyia dome, Safwan dome, and the eastern flank between the two domes (Fig. 4). Magnetic Resonance Image (NMR) and Gamma Ray Logs from wells ZB-X16, X23, X26, X41, X53, and X74 were analyzed using Techlog ™ (Fig. 5 to Fig. 9) to determine reservoir characteristics such as rock types, pore throat radius, and flow units through the Lucia procedure, Winland method, and FZI correlations.

Core data from wells ZB-X53 and ZB-X74 were employed to identify lithological descriptions and to improve the overall results. Additionally, the carbonate content within the samples was estimated by AUTOCALCIMETER.

4- Results

The plots of rock types were obtained by the Lucia procedure for all six wells as shown in Fig. 10.

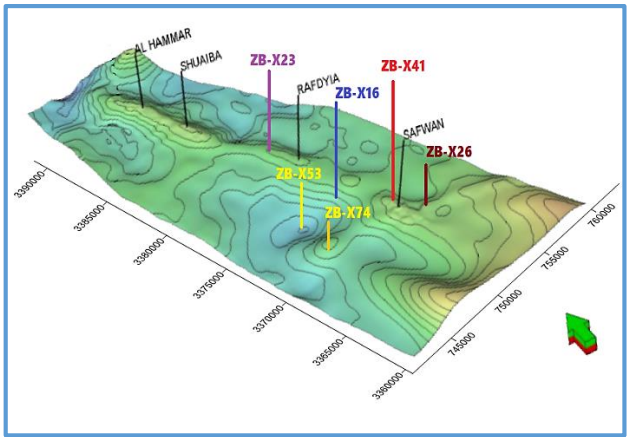

Fig. 4. Wells location in Mishrif Formation Contour Map of Zubair Oilfield

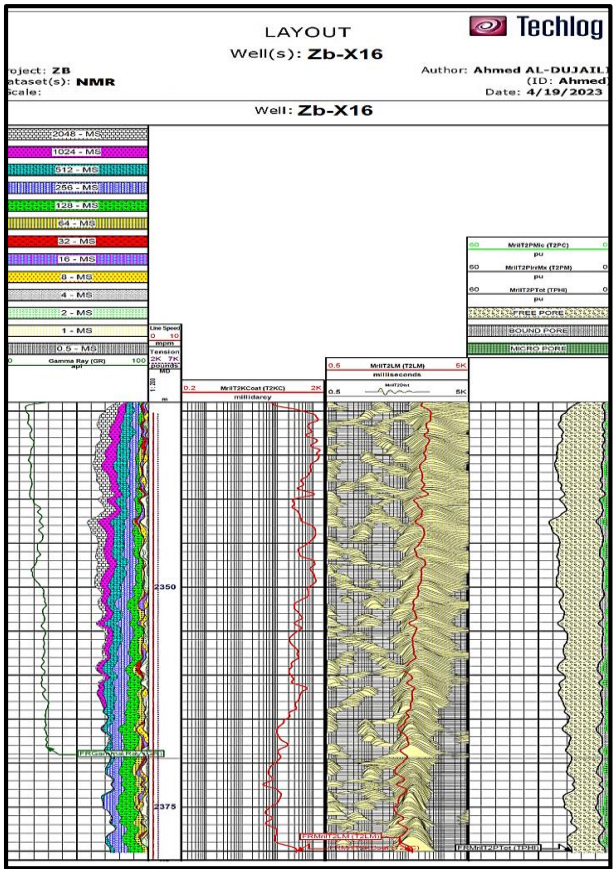

Fig. 5. NMR for the Well Zb-X16 from Depth 2329 to 2381 m

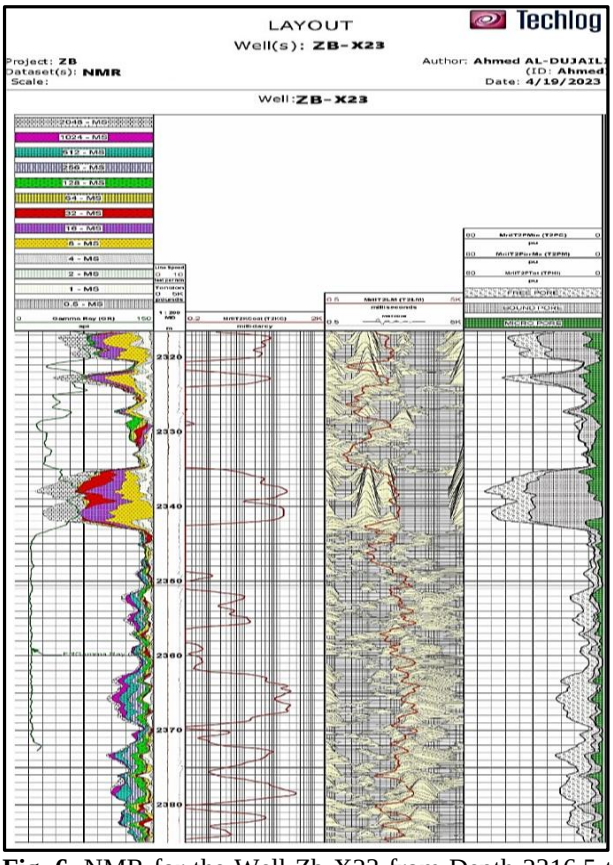

Fig. 6. NMR for the Well Zb-X23 from Depth 2316.5 to 2385 m

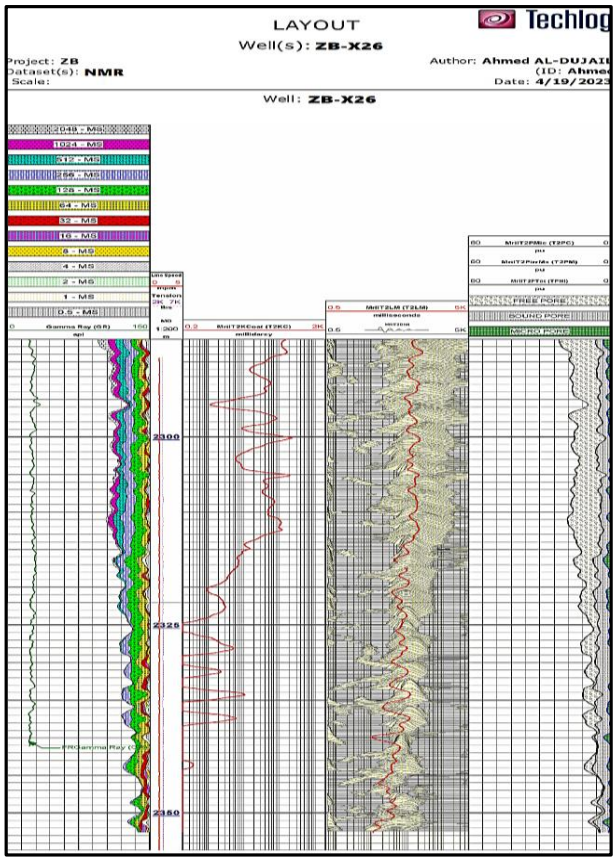

Fig. 7. NMR for the Well Zb-X26 from Depth 2287 to 2352.5 m

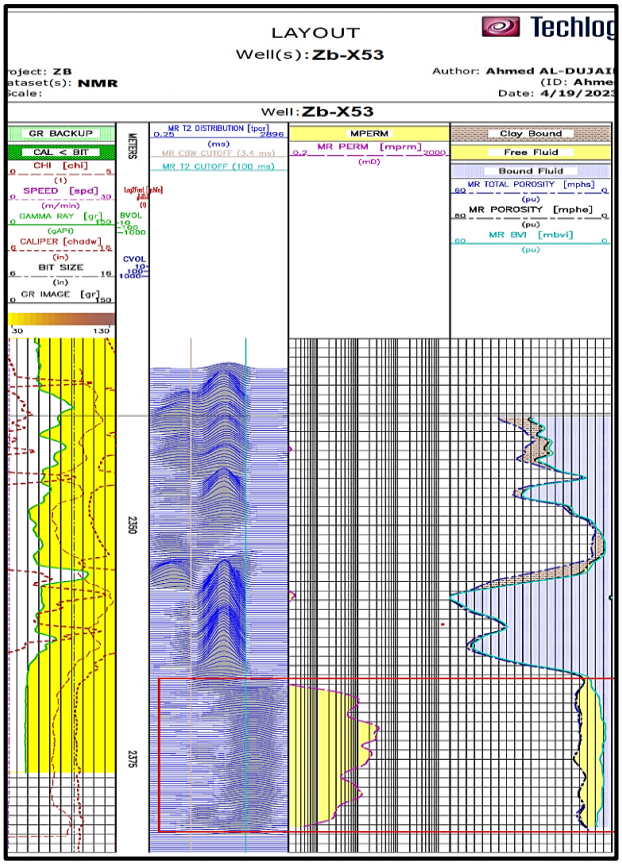

Fig. 8. NMR for the Well Zb-X53 from Depth 2340 to 2383 m

The pore throat radius for all six wells was obtained by the Winland method shown in Fig. 11. Flow units for all six wells can be obtainable by the FZI correlations as shown in Fig. 12.

The stratigraphic column may vary within the Zubair field, so a well-specific lithological column was extracted from core data observation and analysis.

The well-specific geological prognosis column contains also the expected true vertical depth subsea (TVDSS), true Vertical Depth referenced to the Rotary Table (TVDRT), and uncertainty (Table 3 and Table 4).

Fig. 13 shows the Calcimetry results obtained from the Autocalcimeter to measure the carbonate content (limestone and dolomite) for each depth according to the core analysis for the wells ZB- (X53 and X74).

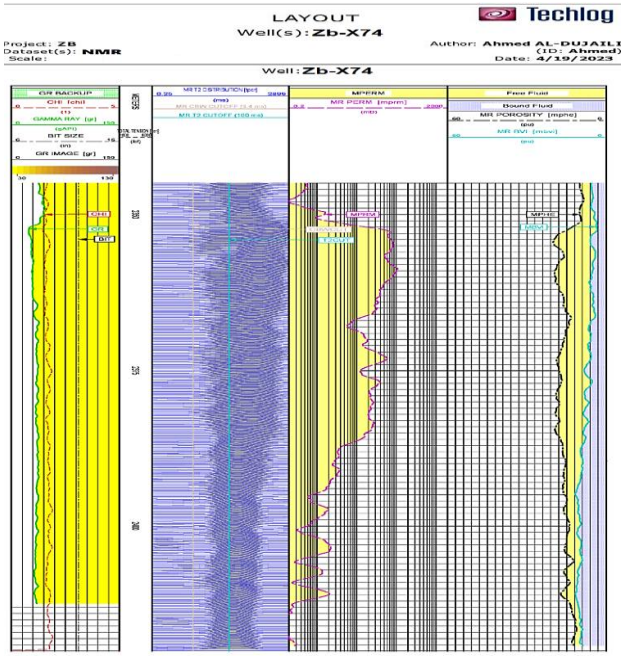

Fig. 9. NMR for the Well Zb-X74 from Depth 2345 to 2421 m

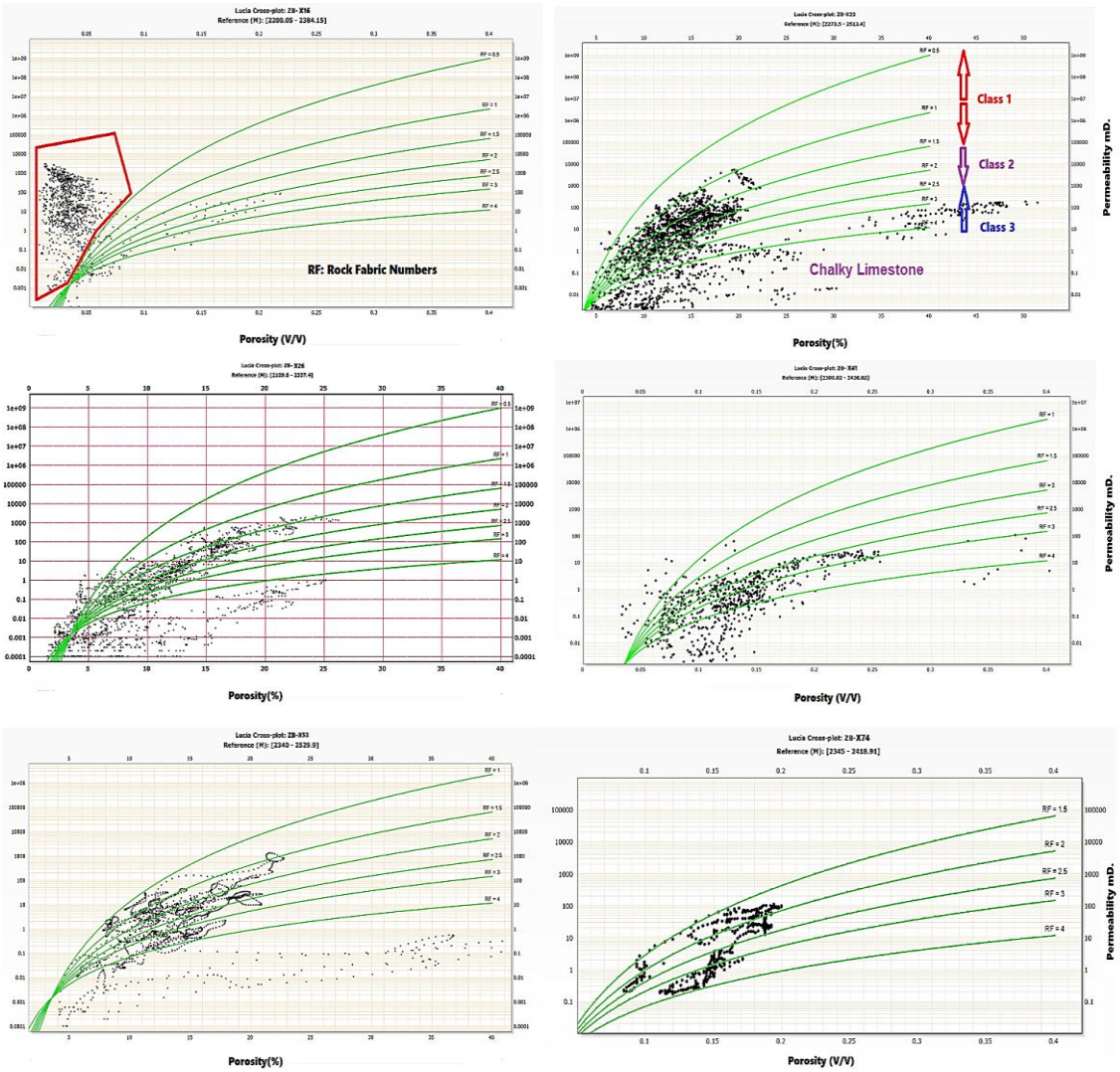

Fig. 10. Rock Type for the Wells ZB- (X16, X23, X26, X41, X-53, and X74) by NMR Data

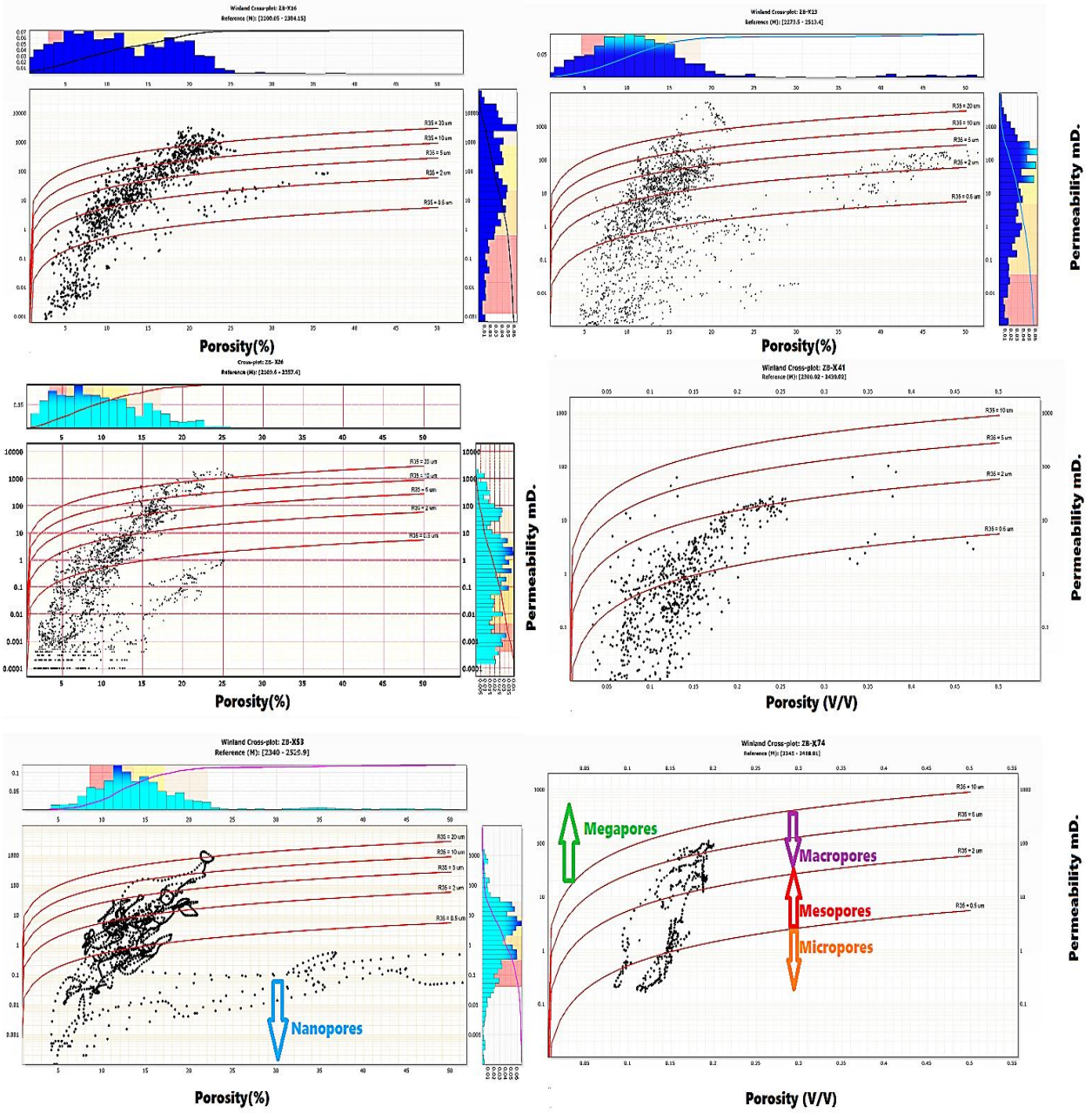

Fig. 11. Pore Throat Radius by Winland Cross Plot for the Wells ZB- (X16, X23, X26, X41, X-53, and X74)

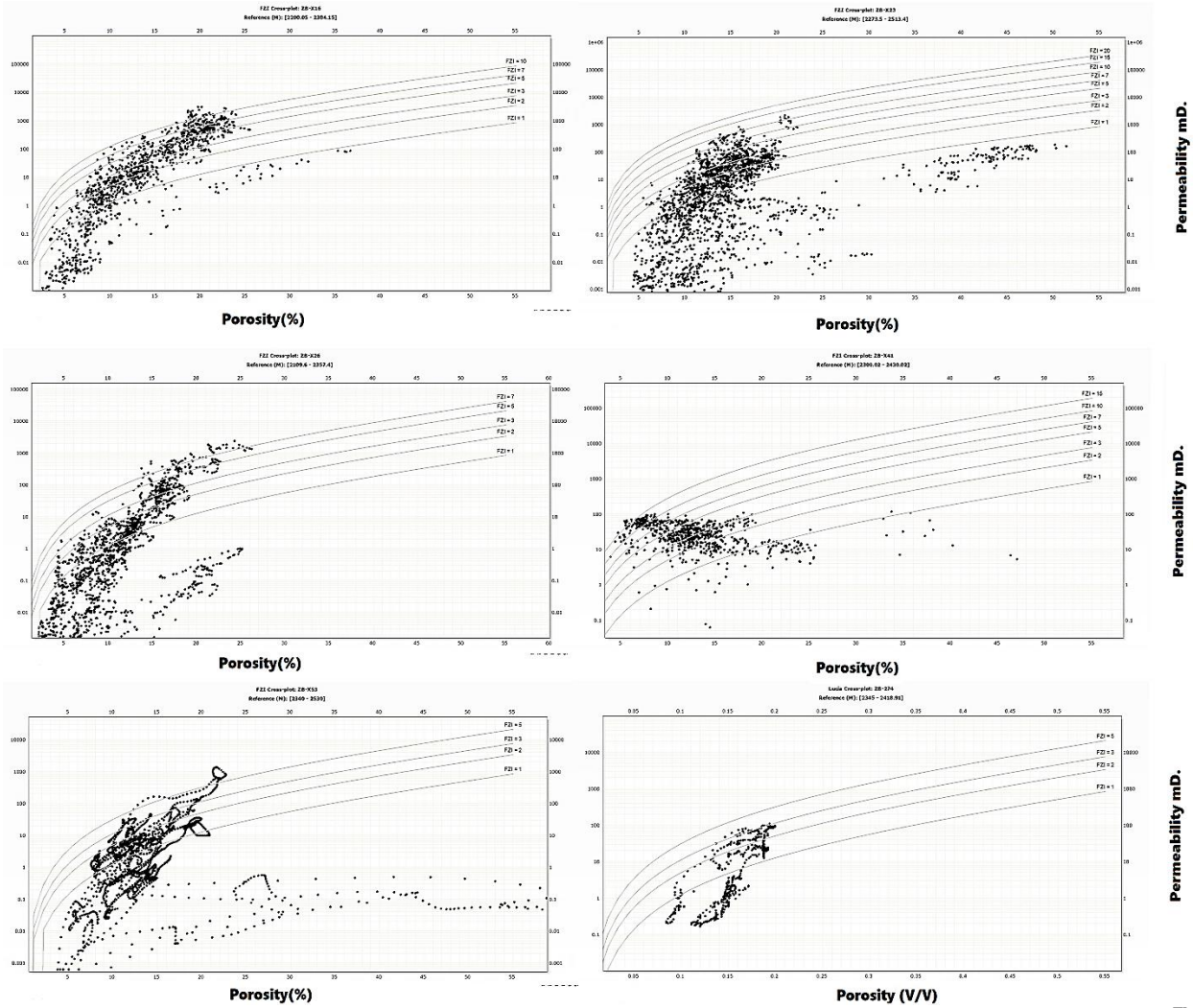

Fig. 12. Flow Units for the Wells ZB- (X16, X23, X26, X41, X-53, and X74) by FZI Correlations Using Techlog ™

Table 3. Lithological Description for the Well ZB-X53 by Core Analysis

Sample depth (m)	SAMPLE DESCRIPTION
2340 – 2410	**Limestone: (100%):** Grainstone, packstone, white, yellowish white, pale yellow, very pale orange, light grey, hard to very hard, soft in parts, irregular, sub blocky, very fine crystalline, with pyrite, fair visible inter-granular porosity. Good trace oil show, dark brown pinpoint oil stain, bright yellow fluorescence, medium blooming light blue cut fluorescence, very thick blue, white residual ring with ultraviolet, a very thin light-yellow residual ring with natural light.
2410 – 2440	**Limestone: (100%):** Grainstone, packstone, white, yellowish white, pale yellow, very pale orange, hard to very hard, soft in parts, irregular, sub blocky, very fine crystalline, poor visible inter-granular porosity, no oil shows
2440 – 2460	**Limestone: (100%):** Wackestone, packstone, white, yellowish white, pale yellow, very pale orange, light grey in parts, hard to very hard, soft in parts, irregular, sub blocky, very fine crystalline, no visible porosity, no oil shows
2460 – 2510	**Limestone: (30%):** Wackestone, packstone, white, yellowish white, pale yellow, very pale orange, light grey in parts, hard to very hard, soft in parts, irregular, sub blocky, very fine crystalline, no visible porosity, no oil shows. **Limestone: (70%):** Mudstone, white, milky white, soft to moderately hard, blocky to sub blocky, Chalky, no visible porosity, no oil shows
2510 – 2540	**Limestone: (10%):** Wackestone, packstone, white, yellowish white, pale yellow, very pale orange, occ. light grey in parts, hard to very hard, soft in parts, irregular, sub-blocky, very fine crystalline, no visible porosity, no oil shows. **Limestone: (90%):** Mudstone, white, milky white, soft to moderately hard, blocky to sub-blocky, Chalky, no visible porosity, no oil shows

Table 4. Lithological Description for the Well ZB-X74 by Core Analysis

Sample depth (m)	SAMPLE DESCRIPTION
2193-2245	**Limestone (60-80%):** Wackestone, Packstone, white, light brown, light grey, medium grey, soft to firm, moderately hard, sub blocky, crypto crystalline to microcrystalline, slightly Argillaceous, no visual porosity, no oil shows. **Shale (40-20%):** Light grey, greenish grey, medium grey, firm to slightly hard, occasionally blocky, fissile, splintery, and calcareous.
2245-2330	**Limestone (100%):** Wackestone, Packstone, white, light yellowish-grey, light brown, pa light yellowish brown, firm to moderately hard, sub blocky, occasionally blocky, microcrystalline, crypto crystalline in part, non to slightly argillaceous, chalky, poor visual porosity. **SHOWS:** Light bright oil stain, brown yellow even fluorescence, streaming bluish white cut fluorescence, thin bluish white residual ring under UV, thick light yellow residual ring natural light, weak oil.
2330-2360	**Limestone (100%):** Wackestone, Packstone, occasionally Grainstone, white, light yellowish-grey, olive grey, light brown, pa yellowish brown, firm to moderately hard, sub blocky, occasionally blocky, cryptocrystalline to microcrystalline, fine crystalline in part, chalky, poor visual porosity. **SHOWS:** Light bright oil stain, bright yellow even fluorescence, slow streaming bluish white cut fluorescence, thin bluish white residual ring under UV, thick light yellow residual ring NL, weak oil.
2360-2395	**Limestone (100%):** Mudstone, Wackstone, Packstone, white, yellowish grey, light yellowish grey, olive grey, light brown, soft, firm to moderately hard, blocky, sub blocky in part, cryptocrystalline to microcrystalline, chalky, slightly Argillaceous, Traces of Shale, poor visual porosity. **SHOWS:** Light brown oil stain, light yellow patchy fluorescence, slow streaming white cut fluorescence, thin white residual ring under UV, very thin light-yellow residual ring NL, weak oil.
2395-2408	**Limestone (100%):** Wackstone, Packstone, light yellowish-grey, olive grey, occasionally brown, pa yellowish brown, hard to moderately hard, sub blocky, occasionally blocky, microcrystalline, crypto crystalline in part, chalky, poor visual porosity, no oil.

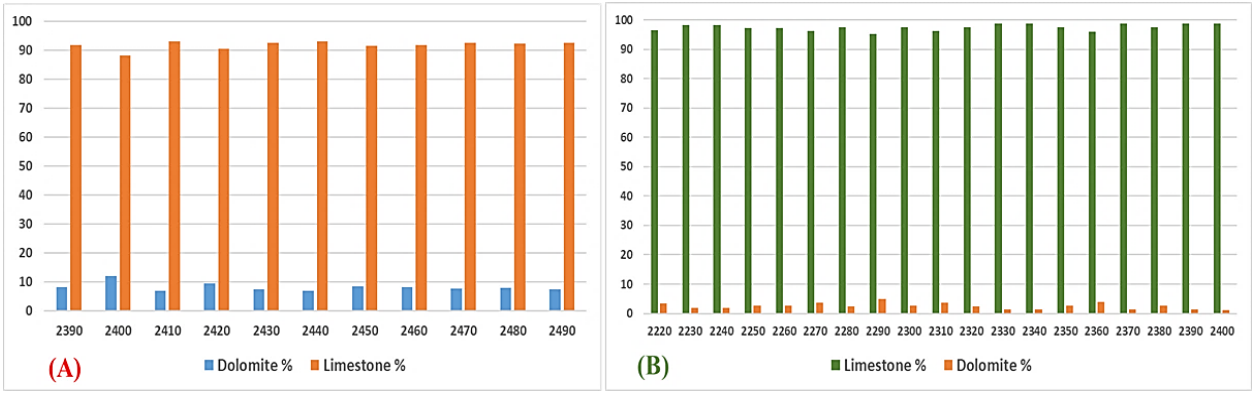

Fig. 13. Limestone and Dolomite Percentages from Autocalcimeter Analysis of Cores for the Wells A- (Zb-X53) and B- (Zb-X74)

5- Discussion

High permeability with moderate porosity values was characterized in the Rafdyia dome, while lower average permeability values in Safwan than in the Rafdyia dome with moderate porosity values were observable.

Petrophysical calculations using NMR data confirm that the porosity values of the lower Mishrif Formation (mb1, mB2, and mC) are higher than the Middle, and the Middle

Mishrif is higher than the Upper Mishrif (mA) in the two Domes. The permeability values of the Upper Mishrif of Safwan Dome are higher than the Rafdyia Dome, which may be due to the karst phenomena in Safwan Dome.

From the results of Lucia's correlations, it is clear that a chalky limestone rock type exists in the vertical line 730000 east along the Zubair Field. This rock type also exists in the well Zb-X53, but another line for the chalky limestone rock cannot be assumed unless another offset well/s is inspected for this objective.

The Mishrif Formation displays heterogeneity, which has an impact on relative permeability, capillary pressure, and recovery factor [42, 43]. This heterogeneity is due to variations in pore throat radius, which affect petrophysical properties. Fig. 10 shows that reservoir rock types range from high porosity-high permeability (Vuggy and melodic flow units) to high porosity-low permeability (high storage and low flow units, which represent microporosity). These differences can be observed more prominently in wells on the flank (Zb-X53 and X-74). Non-reservoir units (barriers and baffles) have low porosity and permeability in their pore throats.

The permeability values will reduce in the trend from the north to south and from the crest to the west flank.

According to the results explained in Fig. 12, the flow units of Mishrif Formation in Rafdyia Dome consisted of ten flow units regardless of the location (North or South).

In Safwan Dome, flow units at the top of the dome are double those on the East flank. In addition, low reservoir characterizations were noticeable in the West flank of the Field (only five flow units).

Fig. 9 for NMR of the well (Zb-X53) shows low permeability with good porosity values for depths from 2340 to 2367 m, which reflects low reservoir quality at the top of Mishrif Formation, which explains why the wells at the flank of the Field have few flow units. That will be supported by Fig. 9, which indicates that good reservoir properties exist at the bottom of the formation.

The Mega-pores exist only in the Rafdyia Dome, while these pores vanish gradually toward the south (Safwan Dome) and to the west flank.

As shown in Fig. 13 and from the results of the Autocalcimeter, carbonate content is more dominant than dolomite in the Mishrif Formation. This dominancy increases in the deep rather than shallow wells according to the high Mg/Ca content ratio in these wells due to the deposition environment.

For comparison, according to Fig. 11 and Fig. 13, dolomitization and dissolution increase pore connectivity and pore throat sizes, and when the dolomite/carbonate percentage rises in the study area (for a specific rate), the reservoir quality increases.

According to the core analysis in Table 3 and Table 4 and the NMR (Fig. 8 and Fig. 9) for wells Zb-X53 and Zb-X74, it is clearly showing that when the wells located in the Zubair Field flank, the Lower Mishrif intervals will have the essential reserves of oil while the Upper Mishrif haven't.

Based on the Reservoir Description log (RDT-GR) in Fig. 5, Fig. 6, and Fig. 14, Mishrif Reservoir shows better reservoir characteristics (high permeability and high porosity) toward the south (ZB-X16) than the north for the Rafdyia dome (ZB-X23).

The same characterizations shown in the Rafdyia dome will extend to cover the Safwan dome, where the well Zb-X26 (Fig. 7 and Fig. 15) showed good reservoir characterizations in the Upper Mishrif.

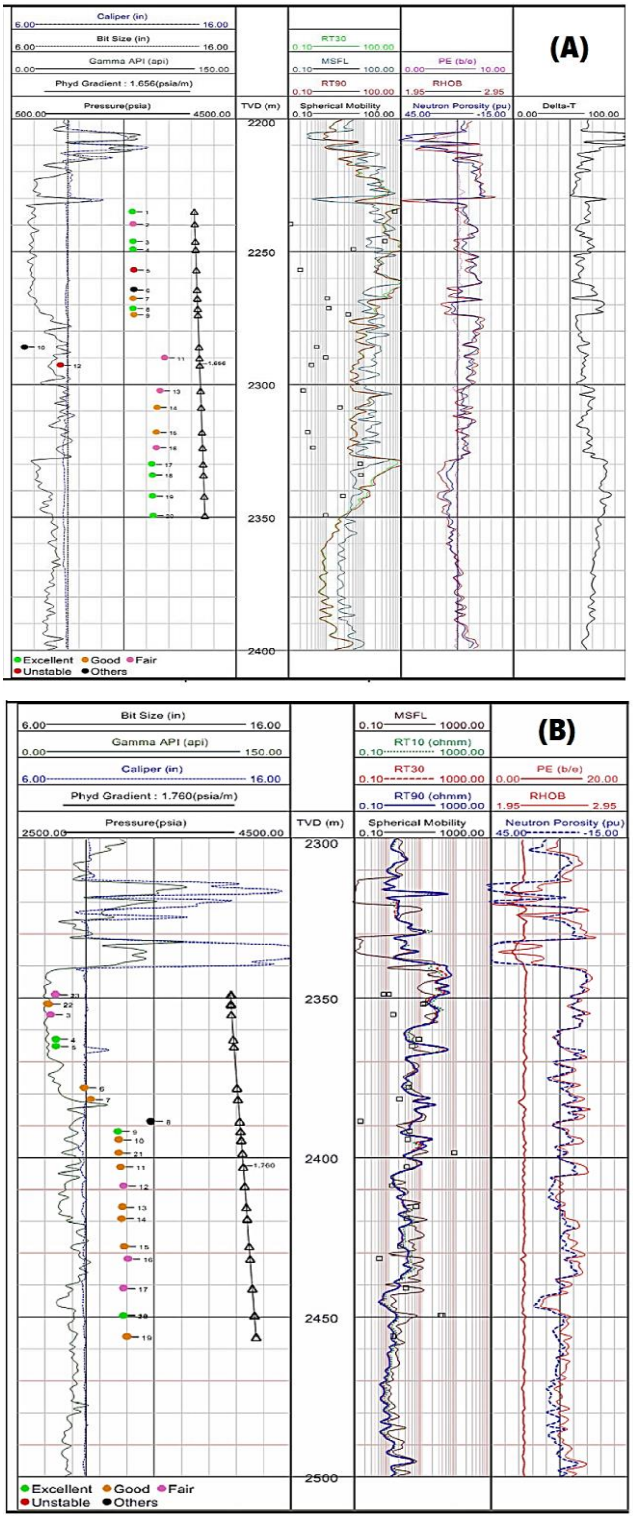

Fig. 14. Reservoir Description Log (RDT-GR) for the Wells A- Zb-X16, B-Zb-X23

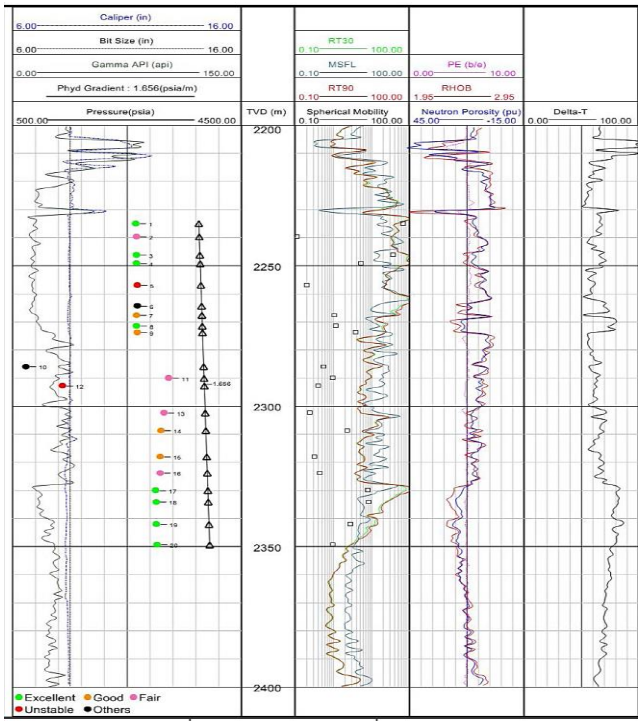

Fig. 15. Reservoir Description Log (RDT-GR) for the Well Zb-X26

6- Conclusions

This study involved the relationship between petrophysical properties (porosity and permeability) using core data and then correlating the result with NMR to determine rock type, pore throat radius, flow units, and reservoir description for Rafdyia and Safwan Domes as follows:

1. The rock types in the Safwan Dome (wells Zb-X41 and Zb-X26) ranged from pack-wackestone, wackestone, and mudstone. The Rafdyia Dome (wells Zb-X16 and Zb-X23) represented packstone to grainstone with few parts of wackestone marked as a shoal and rudist bioherm facies.
2. The rock types of the wells on the west flank (ZB-X53 and Zb-X74) consist of pack-wackestone, wackestone, and some parts of mudstone.
3. The pore throat type in the Safwan Dome can be identifiable mainly as Micropores to Nanopores. Rafdyia Dome represents Megapores and Macropores with Mesoporous throwback at the medium energy level. Packstone microfacies are dominated by back-shoal. Microporous (mainly wackestone) symbolizes lagoon and mid-ramp facies. The Pore throat types that dominated in the west flank are Mesoporous and Micropores.
4. Flow units can be determined as fifteen at the north and seven at the south of the Safwan dome. The Rafdyia Dome has ten flow units in the north and south regions, while the units on the west flank of Zubair Field are five.
5. The Pore throat heterogeneity in the Mishrif Formation is the control factor of the fluid flow conductivity affected by the type of pore size distribution and pore throat size.
6. Mishrif Formation consists of about 90% Limestone and 10% Dolomite in the west flank. The percentage of Limestone will increase toward the west with an increase in the Shale percentage and a decrease in Dolomite.

The best reservoir characterizations appear when the Mishrif Formation extends toward the south trend at the Rafdyia Dome. Again, this description will be better in the same direction for Safwan Dome.

In the west flank of the field, the reservoir characterizations will be better when the formation trends from the north to the south.

Nomenclature

BVI	Bulk Volume Irreducible
BVM	Bulk Volume Movable
FZI	Flow Zone Indicator
GR	Gamma Ray Log
K	permeability (millidarcy)
MREX	Magnetic Resonance Explorer
MRF	Markov random field methods
MRIL	Magnetic Resonance Image Log
NMR	Nuclear Magnetic Resonance
R35	Saturation of Mercury in 35%
RFN	Rocks Fabric Number
RQI	Reservoir Quality Index
TVDSS	true vertical depth subsea
TVDRT	True Vertical Depth referenced to Rotary Table
ZB	Zubair Field
φ_e	Effective porosity (V/V)
φ_z	Ratio of pore volume to grain volume

References

[1] F. J. Lucia, “Petrophysical parameters estimated from visual descriptions of carbonate rocks: A field classification of carbonate pore space,” *Journal of Petroleum Technology*, vol. 35, no. 03, pp. 629–637, Mar. 1983, https://doi.org/10.2118/10073-PA

[2] C. E. Manning and S. E. Ingebritsen, “Permeability of the continental crust: Implications of geothermal data and metamorphic systems,” *Reviews of Geophysics*, vol. 37, no. 1, pp. 127–150, Feb. 1999, https://doi.org/10.1029/1998RG900002

[3] X. Cui, R. M. Bustin, R. Brezovski, B. Nassichuk, K. Glover, and V. Pathi, “A new method to simultaneously measure In-Situ permeability and porosity under reservoir conditions: Implications for Characterization of Unconventional gas Reservoirs,” *All Days*, Oct. 2010, https://doi.org/10.2118/138148-MS

[4] Z. Zhang, H. Zhang, J. Li, and Z. Cai, “Permeability and porosity prediction using logging data in a heterogeneous dolomite reservoir: An integrated approach,” *Journal of Natural Gas Science and Engineering*, vol. 86, p. 103743, Feb. 2021, https://doi.org/10.1016/j.jngse.2020.103743

[5] J. Kozeny "Uber kapillare Leitung der Wasser in Boden. Sitzungsber". *Akad Wiss Wien* 136, 271–306, 1927.

[6] L. M. Schwartz and J. R. Banavar, "Transport properties of disordered continuum systems," *Physical Review. B, Condensed Matter*, vol. 39, no. 16, pp. 11965–11970, Jun. 1989, https://doi.org/10.1103/PhysRevB.39.11965

[7] Y. Yang and A. C. Aplin, "Influence of lithology and compaction on the pore size distribution and modelled permeability of some mudstones from the Norwegian margin," *Marine and Petroleum Geology*, vol. 15, no. 2, pp. 163–175, Mar. 1998, https://doi.org/10.1016/S0264-8172(98)00008-7

[8] Y. Yang and A. C. Aplin, "A permeability–porosity relationship for mudstones," *Marine and Petroleum Geology*, vol. 27, no. 8, pp. 1692–1697, Sep. 2010, https://doi.org/10.1016/j.marpetgeo.2009.07.001

[9] R. C. George, L. Xiao and G. P. Manfred "*NMR Logging Principles and Applications*", Halliburton Energy Services (Halliburton Energy Services Publication, USA). p 251, 1999.

[10] W. E. Kenyon et al., "A Laboratory Study of Nuclear Magnetic Resonance Relaxation and its Relation to Depositional Texture and Petrophysical Properties — Carbonate Thamama Group, Mubarraz Field, Abu Dhabi," *All Days*, Mar. 1995, https://doi.org/10.2118/29886-MS

[11] R. L. Kleinberg, "Utility of NMR T2 distributions, connection with capillary pressure, clay effect, and determination of the surface relaxivity parameter ρ2," *Magnetic Resonance Imaging*, vol. 14, no. 7–8, pp. 761–767, Jan. 1996, https://doi.org/10.1016/S0730-725X(96)00161-0

[12] G. R. Coates, L. Xiao, and M. G. Prammer, *NMR logging: principles and applications*. 1999.

[13] S. H. Al-Mahrooqi, C. A. Grattoni, A. K. Moss, and X. D. Jing, "An investigation of the effect of wettability on NMR characteristics of sandstone rock and fluid systems," *Journal of Petroleum Science & Engineering*, vol. 39, no. 3–4, pp. 389–398, Sep. 2003, https://doi.org/10.1016/S0920-4105(03)00077-9

[14] H. Westphal, I. Surholt, C. Kiesl, H. F. Thern, and T. Kruspe, "NMR Measurements in Carbonate Rocks: Problems and an Approach to a Solution," *Pure and Applied Geophysics*, vol. 162, no. 3, pp. 549–570, Mar. 2005, https://doi.org/10.1007/s00024-004-2621-3

[15] C. Dahai, et al. "Effective porosity, producible fluid and permeability in carbonates from NMR logging." *SPWLA Annual Logging Symposium*. SPWLA, 1994.

[16] M. D. Hürlimann and D. D. Griffin, "Spin dynamics of Carr–Purcell–Meiboom–Gill-like sequences in grossly inhomogeneous B0 and B1 fields and application to NMR well logging," *Journal of Magnetic Resonance*, vol. 143, no. 1, pp. 120–135, Mar. 2000, https://doi.org/10.1006/jmre.1999.1967

[17] P. R. J. Connolly et al., "Simulation and experimental measurements of internal magnetic field gradients and NMR transverse relaxation times (T2) in sandstone rocks," *Journal of Petroleum Science & Engineering*, vol. 175, pp. 985–997, Apr. 2019, https://doi.org/10.1016/j.petrol.2019.01.036

[18] D. G., Robin A. In vivo NMR spectroscopy: principles and techniques. *John Wiley & Sons*, 2019.

[19] NMR interpretation Manual (Paradigm TM Geophysical), chapter 1, 6 and 7, 2013.

[20] M. D. Abdulkadhim, "Porosity and permeability calculation using NMR logging in an Iraqi oil field," IOP Conference Series. *Materials Science and Engineering*, vol. 579, no. 1, p. 012034, Jul. 2019, https://doi.org/10.1088/1757-899X/579/1/012034

[21] A. N. Al-Dujaili, M. Shabani, and M. S. Al-Jawad, "Characterization of flow units, rock and pore types for Mishrif Reservoir in West Qurna oilfield, Southern Iraq by using lithofacies data," *Journal of Petroleum Exploration and Production Technology*, vol. 11, no. 11, pp. 4005–4018, Sep. 2021, https://doi.org/10.1007/s13202-021-01298-9

[22] A. N. Al-Dujaili, M. Shabani, and M. S. Al-Jawad, "Lithofacies, deposition, and clinoforms characterization using detailed core data, nuclear magnetic resonance logs, and modular formation dynamics tests for mishrif formation intervals in West Qurna/1 oil Field, Iraq," *SPE Reservoir Evaluation & Engineering*, vol. 26, no. 04, pp. 1258–1270, Apr. 2023, https://doi.org/10.2118/214689-PA

[23] A. N. Al-Dujaili, "Reservoir rock typing and storage capacity of Mishrif Carbonate Formation in West Qurna/1 Oil Field, Iraq," *Carbonates and Evaporites*, vol. 38, no. 4, Nov. 2023, https://doi.org/10.1007/s13146-023-00908-3

[24] A. Jafarian et al., "Paleoenvironmental, diagenetic, and eustatic controls on the Permo–Triassic carbonate–evaporite reservoir quality, Upper Dalan and Kangan formations, Lavan Gas Field, Zagros Basin," *Geological Journal*, vol. 53, no. 4, pp. 1442–1457, Jul. 2017, https://doi.org/10.1002/gj.2965

[25] L. F. Jerry. "Limestone reservoirs." *Carbonate Reservoir Characterization: An Integrated Approach* 2007, https://doi.org/10.1007/978-3-540-72742-2

[26] H. D. Winland "Evaluation of gas slippage and pore aperture size in carbonate and sandstone reservoirs: *Amoco Production Company Report* F76-G-5, 25 p." Tulsa, Oklahoma 1976.

[27] A. Soleymanzadeh, S. Parvin, and S. Kord, "Effect of overburden pressure on determination of reservoir rock types using RQI/FZI, FZI* and Winland methods in carbonate rocks," *Petroleum Science*, vol. 16, no. 6, pp. 1403–1416, Jun. 2019, https://doi.org/10.1007/s12182-019-0332-8

[28] N. A. J. M. S. T, "Characterization of petrophysical flow units in carbonate reservoirs," *AAPG Bulletin*, vol. 81 Jan. 1997, https://doi.org/10.1306/522b482f-1727-11d7-8645000102c1865d

[29] G. W. Gunter, J. M. Finneran, D. J. Hartmann, and J. D. Miller, "Early determination of reservoir flow units using an integrated petrophysical method," *SPE*, 1997. https://doi.org/10.2118/38679-MS

[30] A. Abedini and F. Torabi, "Pore size determination using normalized J-function for different hydraulic flow units," *Petroleum*, vol. 1, no. 2, pp. 106–111, Jun. 2015, https://doi.org/10.1016/j.petlm.2015.07.004

[31] J. O. Amaefule, M. Altunbay, D. Tiab, D. G. Kersey, and D. K. Keelan, "Enhanced reservoir description: Using core and log data to identify hydraulic (Flow) units and predict permeability in uncored Intervals/Wells," *OnePetro*, 1993, https://doi.org/10.2118/26436-MS

[32] Lazim, Aymen Adil, Muhanad Maki, and Shimam Tariq. "Detect faults of Zubair and Mishrif Formations–Zubair Oilfield by Integrate Structural Geology and Pressure Transient Analyses (PTA) to Selected Wells." *IOSR Journal of Applied Geology and Geophysics* (IOSR-JAGG) 8.5, 57-66, 2020.

[33] M. Al-Jaberi, "ELEMENTS DISTRIBUTION FOR THE UPPER SANDSTONE MEMBER OF THE ZUBAIR FORMATION IN ZUBAIR OIL FIELD, SOUTHERN IRAQ," *Iraqi Geological Journal*, vol. 53, no. 1E, pp. 55–74, Jul. 2020, https://doi.org/10.46717/igj.53.1E.5Ry-2020-07-05

[34] A. K. Faraj, H. A. Hussein, and A. A. Al-Hasnawi, "Estimation of internal friction angle for the third section in Zubair Oil Field: a comparison study," *Iraqi Journal of Oil and Gas Researches*, vol. 2, no. 2, pp. 102–111, Oct. 2022, http://doi.org/10.55699/ijogr.2022.0202.1031

[35] M. F. Hussein, et al. "Case Study for Curing Circulation Losses during Primary Cementing Operations Using Fiber Cement in Zubair Field/Iraq." SPE/IADC Middle East Drilling Technology Conference and Exhibition. *SPE*, 2018. https://doi.org/10.2118/189339-MS

[36] A. M. Handhal, S. M. Jawad, and A. M. Al-Abadi, "GIS-based machine learning models for mapping tar mat zones in upper part (DJ unit) of Zubair Formation in North Rumaila supergiant oil field, southern Iraq," *Journal of Petroleum Science & Engineering*, vol. 178, pp. 559–574, Jul. 2019, https://doi.org/10.1016/j.petrol.2019.03.071

[37] A. J. Al-Khafaji, S. J. Yonis, R. N. A. Ibrahim, S. Almarsomi, and F. Sadooni, "Geochemical characterization and origin of the Cretaceous Sa'di, Khasib, Mishrif, and Nahr Umr Crude Oils in Halfaya Oilfield, Southern Mesopotamian Basin, Iraq," *Petroleum Science and Technology*, vol. 39, no. 21–22, pp. 993–1007, Sep. 2021, https://doi.org/10.1080/10916466.2021.1980587

[38] Q. Abeed, D. Leythaeuser, and R. Littke, "Geochemistry, origin and correlation of crude oils in Lower Cretaceous sedimentary sequences of the southern Mesopotamian Basin, southern Iraq," *Organic Geochemistry* (Online), vol. 46, pp. 113–126, May 2012, https://doi.org/10.1016/j.orggeochem.2012.02.007

[39] Z. MHAL, I. A. Almallah, and F. M. Al-Najm. "Petrophysical properties evaluation using well logging of the upper sand member of Zubair Formation in Zubair oil Field, Southern Iraq." *Basrah Journal of Science*, 37.3, 456-480, 2019.

[40] A. N. Al-Dujaili, M. Shabani, and M. S. Al-Jawad, "Identification of the best correlations of permeability anisotropy for Mishrif reservoir in West Qurna/1 oil Field, Southern Iraq," *Egyptian Journal of Petroleum*, vol. 30, no. 3, pp. 27–33, Sep. 2021, https://doi.org/10.1016/j.ejpe.2021.06.001

[41] T. A. Mahdi and A. a. M. Aqrawi, "SEQUENCE STRATIGRAPHIC ANALYSIS OF THE MID-CRETACEOUS MISHRIF FORMATION, SOUTHERN MESOPOTAMIAN BASIN, IRAQ," *Journal of Petroleum Geology*, vol. 37, no. 3, pp. 287–312, Jun. 2014, https://doi.org/10.1111/jpg.12584

[42] A. N. Al-Dujaili, M. Shabani, and M. S. Al-Jawad, "Effect of heterogeneity on capillary pressure and relative permeability curves in carbonate reservoirs. A case study for mishrif formation in West Qurna/1 oilfield, Iraq," *Iraqi Journal of Chemical and Petroleum Engineering*, vol. 24, no. 1, pp. 13–26, Mar. 2023, https://doi.org/10.31699/IJCPE.2023.1.3

[43] A. N. Al-Dujaili, M. Shabani, and M. S. Al-Jawad, "Effect of heterogeneity on recovery factor for carbonate reservoirs. A case study for mishrif formation in West Qurna Oilfield, southern Iraq," *Iraqi Journal of Chemical and Petroleum Engineering*, vol. 24, no. 3, pp. 103–111, Sep. 2023, https://doi.org/10.31699/IJCPE.2023.3.10

التوصيف المكمني والصخري لتكوين المشرف/حقل الزبير (قبتي الرافضية وصفوان) بواسطة الرنين المغناطيسي النووي وتحليل اللباب الصخري

أحمد نوري الدجيلي [١، *]

١ جامعة أمير كبير التكنولوجية، قسم هندسة النفط، ايران

الخلاصة

تعتبر دراسات تحديد خصائص الصخور والمكمن الخلفية الأساسية لفحص كفاءة المكمن من خلال تحديد أنواع الصخور والمسام. للتعرف على الخصائص الصخرية والخزنية لتكوين المشرف في جنوب حقل الزبير (قبتي الرافضية وصفوان). تم استخدام الرنين المغناطيسي النووي (NMR) لستة آبار، اثنان في كل من (قبة الرفدية وصفوان)، واثنين في الجهة الغربية. تم استخدام ارتباطات محددة لوصف تصنيف الصخور وتقدير نصف قطر المسام الحلقي والتعرف على وحدات التدفق المحتملة.

أظهرت النتائج أن تكوين المشرف يتكون بشكل رئيسي من الحجر الجيري والدولوميت والصخر الزيتي. تراوحت أنواع الصخور لقبة صفوان في الغالب بين حزم الحجر الصخري (Wackstone) والحجر الطيني (Mudstone). في الوقت نفسه، تمثل قبة الرافضية حجر الركام إلى حجر الحبوب مع ملاحظة ان بعض الحجر الصخري يمثل سحنة بيولوجية ضحلة ورودية (shoal and rudist bioherm). تتكون أنواع الصخور في الجانب الغربي من رزم الحجر الصخري، والحجر الطيني.

المسام الحلقية لقبة صفوان هي من المسام الصغيرة إلى المسام النانوية بشكل عام، في حين أن قبة الراقضية تتميز بالمسام الكبيرة والدقيقة مع Macropores و Mesoporous. الجانب الغربي لتكوين المشرف في حقل الزبير عبارة عن مسامات متوسطة الحجم ومسام صغيرة. وحدات التدفق لصفوان هي خمس عشرة وحدة شمال القبة وسبع وحدات جنوبها. وفي قبة الرافضية يمكن ملاحظة عشر وحدات جريان في الجزئين الشمالي والجنوبي، كما توجد خمس وحدات جريان في الجانب الغربي من حقل الزبير.

الكلمات الدالة: توصيف الخزان، الرنين المغناطيسي النووي، قبب الرافضية وصفوان، تكوين المشرف، حقل الزبير.